



SERA JRA-6

**EMSC**

**Earthquake Qualitative Impact Assessment**

Improvements and New Performance Evaluation

Reviewed by: Alberto Michelini

Submission date: October 31, 2019

Start date of project

1 January 2017

Duration

36 months

Author

S. Julien-Laferrière



### **Abstract**

This report is the continuation of the previous report [1] on the performance analysis of the impact assessment tool EQIA (Earthquake Qualitative Impact Assessment) developed at the EMSC (European-Mediterranean Seismological Centre) within the NERIES/JRA-3 project. EQIA provides fast and automatic impact assessment for world crustal earthquakes (depth < 40km) with a magnitude of 5 or higher, in order to quickly detect a potentially damaging earthquake.

This report follows the recent rejuvenate of EQIA in Python and the recent improvements implemented, in particular the new population database used: the open access Global Human Settlement (GHS) database, the new rupture length evaluation for  $M \geq 7$  earthquakes and the new approach for uncertainties management.

This new version of EQIA has excellent performance with 99% of correct impact estimations, in particular when using the GHS database (99.5% of correct impact predictions with 76.3 to 90.7% for  $M \geq 7$  event depending on the rupture scenario).

Additionally, the rewriting in Python will greatly ease the maintenance and the future upgrades.

### **Target Audience**

This document is intended for all of SERA members, the seismological community and ARISTOLE partners.

### **Disclaimer**

The European Union and its Innovation and Networks Executive Agency (INEA) are not responsible for any use that may be made of the information any communication activity contains.

The content of this publication does not reflect the official opinion of the European Union. Responsibility for the information and views expressed in the therein lies entirely with the author(s).



# Contents

<b>List of Figures</b>	<b>4</b>
<b>List of Tables</b>	<b>6</b>
<b>Introduction</b>	<b>7</b>
<b>1 New population database</b>	<b>8</b>
1.1 Global Human Settlement . . . . .	8
<b>2 Rupture length equation</b>	<b>10</b>
2.1 Strike slip or dip slip fault type . . . . .	10
2.2 Interplate or Stable Continental Region . . . . .	11
<b>3 Toward reduced uncertainties</b>	<b>12</b>
<b>4 New performance evaluation</b>	<b>14</b>
<b>Conclusion</b>	<b>17</b>
<b>A Execution time</b>	<b>18</b>
<b>Bibliography</b>	<b>19</b>



## List of Figures

- 1.1 EQIA results with the LandScan2015 database for the September 28th, 2018 M7.5 earthquake in Sulawesi, Indonesia (event [715248](#)). The displayed scenario corresponds to an unilateral rupture propagation. On the left, a map of the earthquake location with the population density, as well as the modelled rupture (red line) and the iso-PGA boundaries (in black or red). On the right, the corresponding calculated impact: solid lines represent the model at different population densities, the red point and rectangle the fatalities mean value and uncertainties. 2256 fatalities were recorded for this event (very heavy impact). . . . . 9
- 1.2 EQIA results with the GHS2015 database for the September 28th, 2018 M7.5 earthquake in Sulawesi, Indonesia (event [715248](#)). The displayed scenario corresponds to an unilateral rupture propagation. On the left, a map of the earthquake location with the population density, as well as the modelled rupture (red line) and the iso-PGA boundaries (in black or red). On the right, the corresponding calculated impact: solid lines represent the model at different population densities, the red point and rectangle the fatalities mean value and uncertainties. 2256 fatalities were recorded for this event (very heavy impact). . . . . 9
- 2.1 Rupture length computed for the different equations from [2]. For the sake of comparison, the equation used so far in EQIA. . . . . 11
- 3.1 EQIA results with the GHS2015 database for the September 28th, 2018 M7.5 earthquake in Sulawesi, Indonesia (event [715248](#)). The displayed scenario corresponds to an unilateral rupture propagation. On the left, a map of the earthquake location with the population density, as well as the modelled rupture (red line) and the iso-PGA boundaries (in black or red). On the right, the corresponding calculated impact: solid lines represent the model at different population densities, the red point and rectangle the fatalities mean value and uncertainties. 2256 fatalities were recorded for this event (very heavy impact). . . . . 12
- 3.2 EQIA results with reduced uncertainties with the GHS2015 database for the September 28th, 2018 M7.5 earthquake in Sulawesi, Indonesia (event [715248](#)). The displayed scenario corresponds to an unilateral rupture propagation. On the left, a map of the earthquake location with the population density, as well as the modelled rupture (red line) and the iso-PGA boundaries (in black or red). On the right, the corresponding calculated impact: solid lines represent the model at different population densities, the red point and rectangle the fatalities mean value and uncertainties. 2256 fatalities were recorded for this event (very heavy impact). . . . . 13



- A.1 Average EQIA execution times (over three executions) for the same epicentre coordinates (i.e. the same population distribution) with different magnitude and population databases. These numbers highly depend on the population distribution. . . . . 18



## List of Tables

1	EQIA impact categories. . . . .	7
4.1	EQIA's performance (GHS classic) for 7291 earthquakes (7194 $M < 7$ and 97 $M \geq 7$ ) from January 2010 to May 2019. . . . .	14
4.2	EQIA's performance (GHS reduced) for 7291 earthquakes (7194 $M < 7$ and 97 $M \geq 7$ ) from January 2010 to May 2019. . . . .	15
4.3	EQIA's performance (LandScan classic) for 7291 earthquakes (7194 $M < 7$ and 97 $M \geq 7$ ) from January 2010 to May 2019. . . . .	15
4.4	EQIA's performance (LandScan reduced) for 7291 earthquakes (7194 $M < 7$ and 97 $M \geq 7$ ) from January 2010 to May 2019. . . . .	15
4.5	EQIA's performance before the upgrade (LandScan database, classic uncertainties) for 7268 earthquakes (7171 $M < 7$ and 97 $M \geq 7$ ) from January 2010 to May 2019. . . . .	15



# Introduction

EQIA (Earthquake Qualitative Impact Assessment) has been developed by Gilles et al. [3, 4] within the NERIES/JRA-3 project. Since 2007, it provides fast and automatic impact assessment for crustal earthquakes (depth  $\geq$  40km) with a magnitude of 5 or higher. The purpose of EQIA is to quickly detect a potentially damaging earthquake, depending on its magnitude and on the density of population in the affected region. As part of the SERA JRA-6 project, EQIA, has been rejuvenate in Python as well as improved in several ways. This document is a quick overview of the recent upgrades implemented in EQIA as well as a new performance analysis.

The main improvements that will be discussed in this report are:

- The possibility to use an additional population database
- The new rupture length evaluation
- The new approach for uncertainties

We remind that, in view of the large uncertainties, EQIA does not aim at providing an accurate estimate of the number of casualties due to too large uncertainties but only a range of possible impact. The different impact categories used in EQIA are listed in Tab. 1.

Impact category	Fatalities
None	0
Light	1 to 39
Moderate	40 to 99
Heavy	100 to 999
Very Heavy	1000 to 9999
Extreme	> 10000

Table 1: EQIA impact categories.

The first part of this report will present the new population database introduced in EQIA. Then, the upgrades related to the evaluation of the rupture length will be detailed. The new uncertainties approach proposed for EQIA will be discussed afterwards. The last part of this report will be devoted to the results of the performance evaluation of the new version of EQIA.



# 1 New population database

Currently, EQIA uses the LandScan database [5] (available years: 2007, 2011 and 2015) for evaluating the population distribution around the earthquake epicentre. Since Landscan is not free, we wish to move to an open access database. The Global human Settlement database, by the European Commission, seems a suitable choice.

## 1.1 Global Human Settlement

The Global Human Settlement (GHS)<sup>1</sup> [6, 7] produces global spatial information describing the human presence around the globe over time (1975, 1990, 2000 and 2015). It is an open and free database, supported by the Joint Research Centre (JRC) and the DG for Regional Development (DG REGIO) of the European Commission, and by the international partnership GEO Human Planet Initiative.

Population data is available at different spatial resolutions (WGS84): 9 arcsec (around 250m near the equator) and 30 arcsec (around 1km near the equator). So far, only the last was tested.

The results of EQIA, for the September 28th, 2018 M7.5 earthquake in Sulawesi, Indonesia, are displayed Fig. 1.1 (with LandScan 2015) and 1.2 (with GHS 2015).

As one can see from Fig. 1.1 and 1.2, there are quite big discrepancies between the two databases. In overall the GHS population is much more dense. Since judging the quality of these databases, based on different methods, is beyond the scope of our work, we'll keep both to account for our lack of knowledge and keep a conservative approach. Thus, for each earthquake triggering EQIA, 2 computations will be launched, one with LandScan, the other one with GHS.

It is important to note that GHS aims at making one release per year, which would be a very interesting feature to improve the reliability of the impact prediction.

The execution time of EQIA with the two different databases as input is presented in the Appendix A.

---

<sup>1</sup><https://ghsl.jrc.ec.europa.eu/about.php>

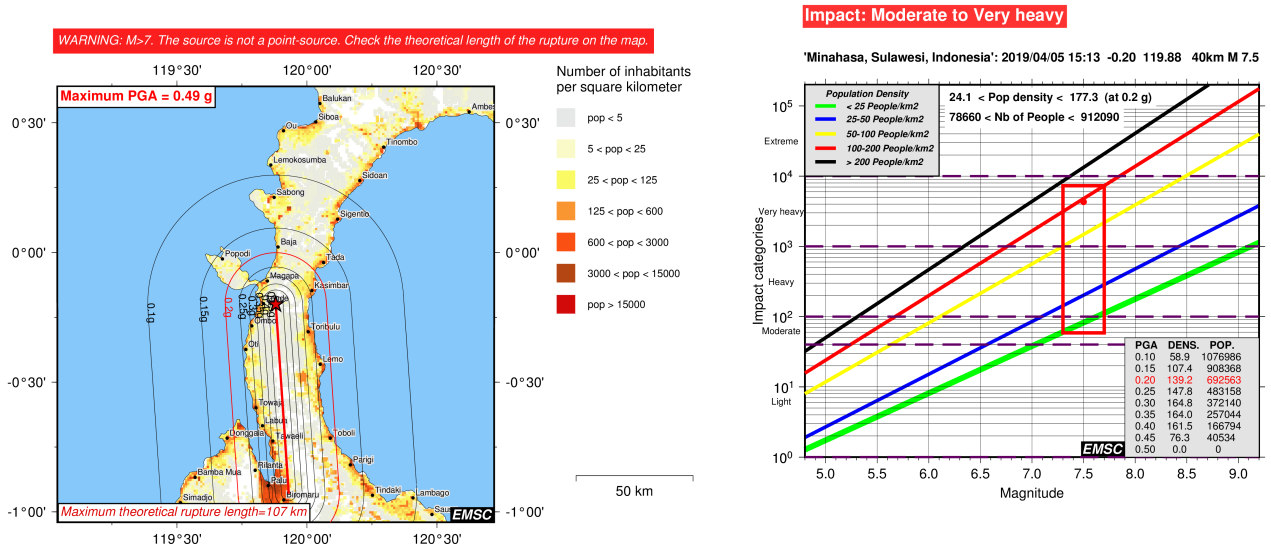


Figure 1.1: EQIA results with the LandScan2015 database for the September 28th, 2018 M7.5 earthquake in Sulawesi, Indonesia (event 715248). The displayed scenario corresponds to an unilateral rupture propagation. On the left, a map of the earthquake location with the population density, as well as the modelled rupture (red line) and the iso-PGA boundaries (in black or red). On the right, the corresponding calculated impact: solid lines represent the model at different population densities, the red point and rectangle the fatalities mean value and uncertainties. 2256 fatalities were recorded for this event (very heavy impact).

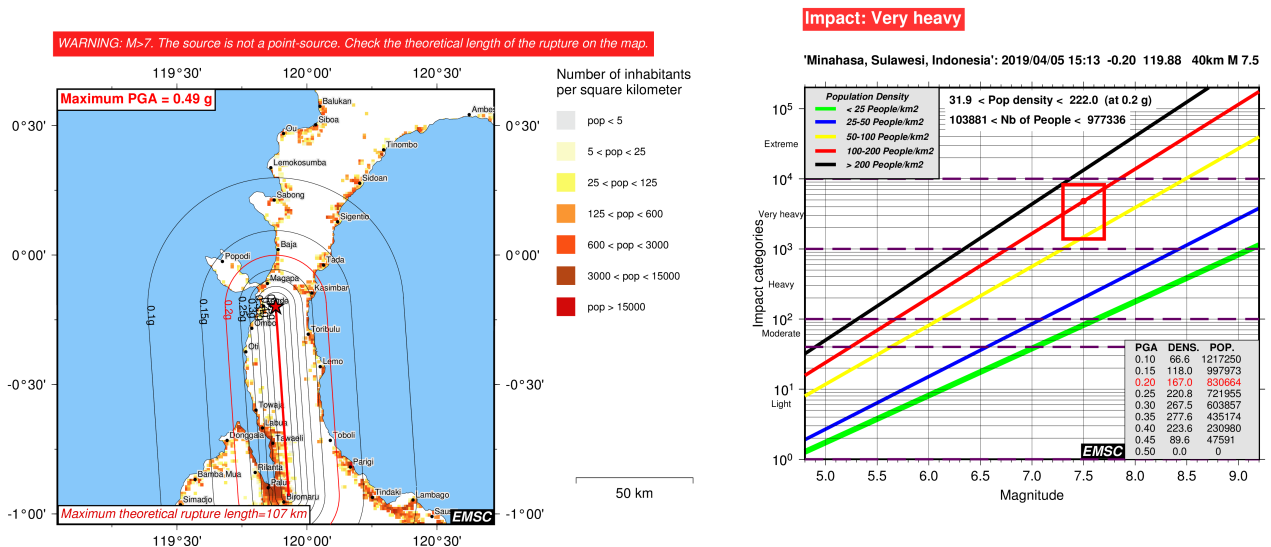


Figure 1.2: EQIA results with the GHS2015 database for the September 28th, 2018 M7.5 earthquake in Sulawesi, Indonesia (event 715248). The displayed scenario corresponds to an unilateral rupture propagation. On the left, a map of the earthquake location with the population density, as well as the modelled rupture (red line) and the iso-PGA boundaries (in black or red). On the right, the corresponding calculated impact: solid lines represent the model at different population densities, the red point and rectangle the fatalities mean value and uncertainties. 2256 fatalities were recorded for this event (very heavy impact).

## 2 Rupture length equation

The rupture length evaluation is key in EQIA since it monitors the size of the impacted zone. For small to medium size earthquakes ( $M < 7$ ) a point source model is enough to represent the rupture. For larger earthquakes ( $M \geq 7$ ), up to now, the rupture length is taken as Eq. 2.1, based on [8].

$$M = 2.44 + 0.59 \cdot \log_{10}(L) \iff L = 10^{(M-2.44)/0.59} \quad (2.1)$$

This equation has been updated with more recent work [2], taking into account the fault type. There are now 4 relations between the rupture length and the magnitude, depending on the fault type:

- Inter-plate dip slip:

$$M = 4.24 + 1.667 \cdot \log_{10}(L) \iff L = 10^{(M-4.24)/1.667} \quad (2.2)$$

- Inter-plate strike slip

$$M = 5.27 + \log_{10}(L) \iff L = 10^{M-5.27} \quad (2.3)$$

- Intra-plate (SCR: Stable Continental Region) dip slip

$$M = 4.32 + 1.667 \cdot \log_{10}(L) \iff L = 10^{(M-4.32)/1.667} \quad (2.4)$$

- Intra-plate strike slip

$$M = \begin{cases} 4.25 + 1.667 \cdot \log_{10}(L) & \text{if } L < 60\text{km} \\ 5.44 + \log_{10}(L) & \text{otherwise} \end{cases} \iff L = \begin{cases} 10^{(M-4.25)/1.667} & \text{if } M < 7.2 \\ 10^{M-5.44} & \text{otherwise} \end{cases} \quad (2.5)$$

The rupture length for these 4 cases as a function of the magnitude is represented Fig. 2.1, the equation used so far in EQIA, Eq. 2.1 is also displayed for the sake of comparison.

### 2.1 Strike slip or dip slip fault type

To determine whether the fault is a dip slip or a strike slip, we need the dip angle,  $\delta \in [0^\circ; 90^\circ]$ , and the slip angle,  $\lambda \in [-180^\circ; 180^\circ]$  (in addition to the strike angle used to determine the rupture orientation). Usually, after 30 to 40 minutes this information is available.

We are considering a strike slip fault if:

- $\lambda \in [-180^\circ; -135^\circ] \cup [-45^\circ; 45^\circ] \cup [135^\circ; 180^\circ]$
- $\delta \geq 70^\circ$

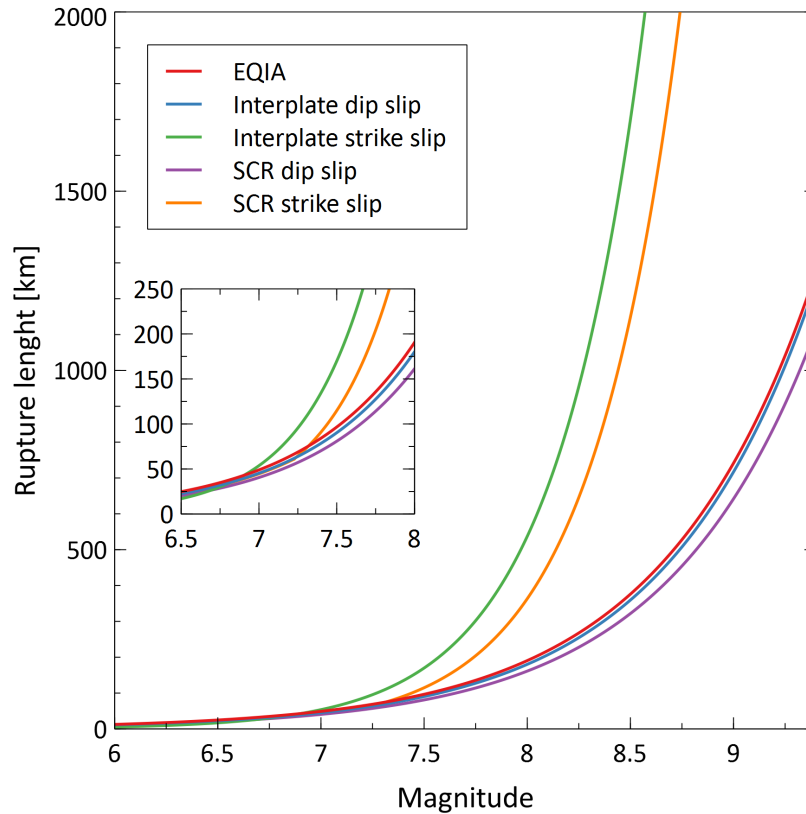


Figure 2.1: Rupture length computed for the different equations from [2]. For the sake of comparison, the equation used so far in EQIA.

Otherwise, we consider a dip slip. If this information is not available, by default we consider a dip slip since they are the most common slips.

## 2.2 Interplate or Stable Continental Region

To determine whether the epicentre is in an interplate zone or in a stable continental region, we check the distance from the epicentre to the nearest plate boundary. For this purpose, we use the boundaries defined by P. Bird [9] and set the limit distance to the maximum rupture length (taking into account the magnitude uncertainty) plus 3 times the typical epicentre location uncertainty (by default, 15km).



### 3 Toward reduced uncertainties

Currently, EQIA takes into account uncertainties on the epicentre location and on the earthquake magnitude. Typical uncertainties are respectively 15km and 0.2, but can be conservative, for example when seismological stations are numerous and well spread around the epicentre. For instance, in the EMSC database, over 85% of the earthquakes magnitude are defined within 0.1 of their final magnitude 20 minutes after they occurred. In the new version of EQIA, EQIA is launched with uncertainties on epicentre location and magnitude of 15km and 0.2 about 10 minutes after the earthquake. At 20 minutes after the earthquake, EQIA is relaunched with reduced uncertainties of 10km and 0.1.

Fig. 3.1 and 3.2 below presents two different computations of EQIA, respectively with typical uncertainties of 15km and 0.2 and reduced uncertainties of 10km and 0.1. Needless to say that the impact assessment precision is much better with reduced uncertainties in inputs. However, this improved precision will decrease EQIA's reliability in predicting the correct impact: with increased accuracy, some errors that have been blurred so far become obvious.

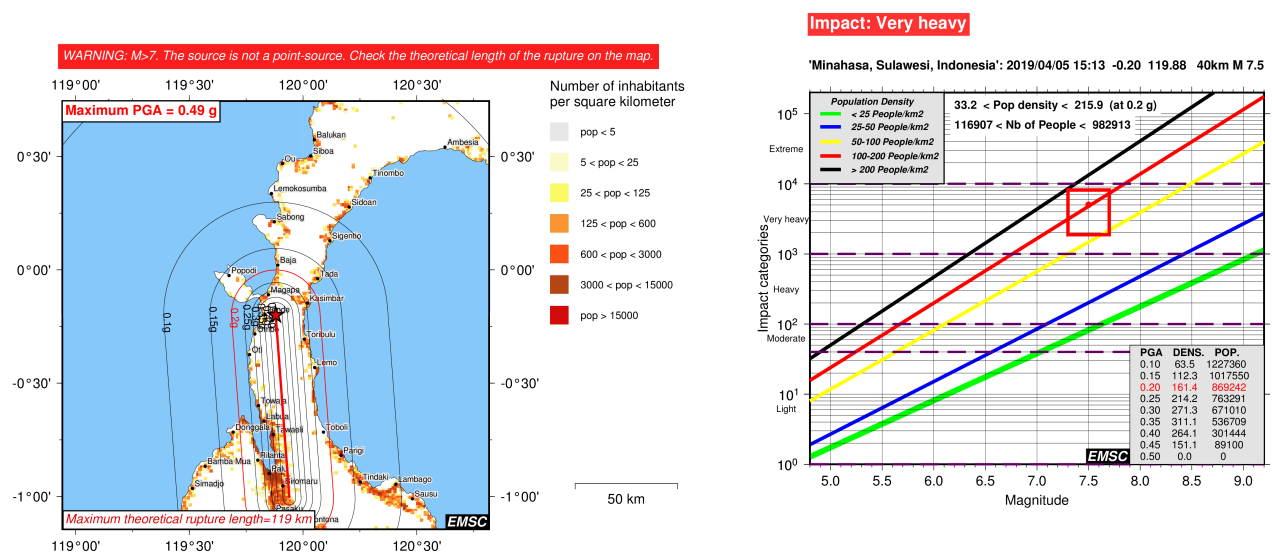


Figure 3.1: EQIA results with the GHS2015 database for the September 28th, 2018 M7.5 earthquake in Sulawesi, Indonesia (event 715248). The displayed scenario corresponds to an unilateral rupture propagation. On the left, a map of the earthquake location with the population density, as well as the modelled rupture (red line) and the iso-PGA boundaries (in black or red). On the right, the corresponding calculated impact: solid lines represent the model at different population densities, the red point and rectangle the fatalities mean value and uncertainties. 2256 fatalities were recorded for this event (very heavy impact).

Furthermore, we plan to add on the visual outputs created with EQIA information on the parameters that could play a major role on the impact assessment (violent earthquake days before inducing population displacement, earthquake occurring during night time etc.) to give a comprehensive view on the limitations of quick impact assessment.

Moreover, as part of the RISE project, a new collaboration with the ETHzürich, around the FinDer algorithm is starting, to exploit the felt reports gathered by the EMSC. This collaboration aims at quickly constrain the

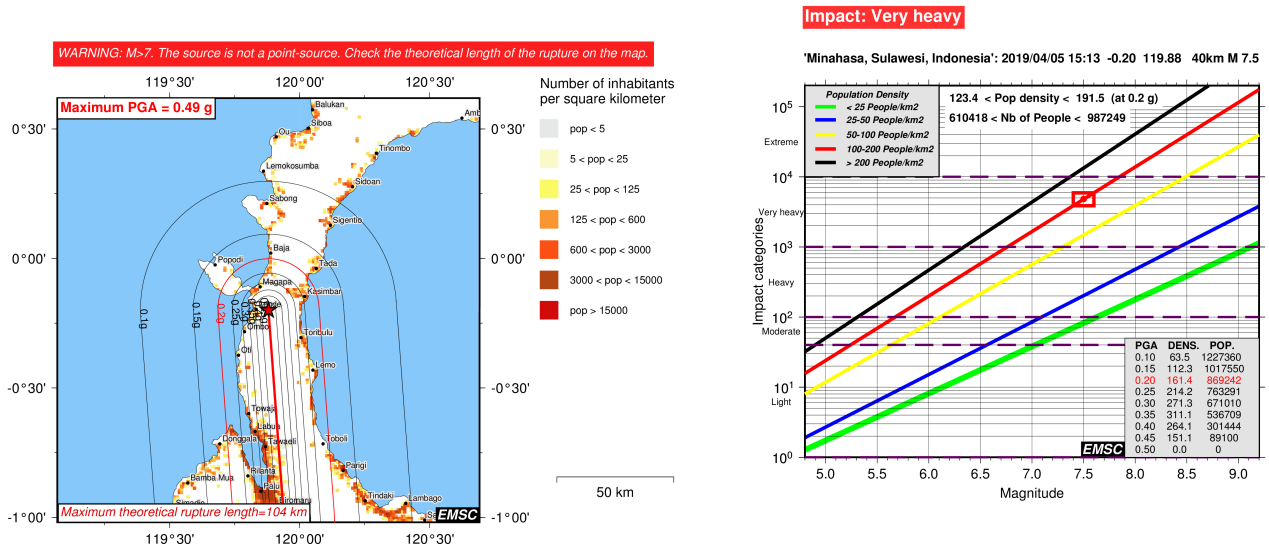


Figure 3.2: EQIA results with reduced uncertainties with the GHS2015 database for the September 28th, 2018 M7.5 earthquake in Sulawesi, Indonesia (event 715248). The displayed scenario corresponds to an unilateral rupture propagation. On the left, a map of the earthquake location with the population density, as well as the modelled rupture (red line) and the iso-PGA boundaries (in black or red). On the right, the corresponding calculated impact: solid lines represent the model at different population densities, the red point and rectangle the fatalities mean value and uncertainties. 2256 fatalities were recorded for this event (very heavy impact).

finite rupture as well as the shaking levels from crowd-sourced data. In particular, it seems very promising to quickly get the fault rupture orientation and propagation since we would be able to promptly evaluate the most realistic scenario when it comes to large earthquakes (when  $M \geq 7$  we consider in EQIA a 1D finite rupture model, please refer to the previous report [1]).

## 4 New performance evaluation

An analysis of the upgraded version of EQIA has been done, similarly to [1] (see the latter for additional information on the analysis). EQIA's performance was assessed by comparing EQIA's impact predictions to the NOAA database [10], considered as the reference. We make the distinction between  $M < 7$  events where the rupture is considered a point source and  $M \geq 7$  events where the rupture is modelled by a line (if at least one nodal plane is known). For  $M \geq 7$  events, 3 endmember rupture propagation scenarios are considered for each nodal plane: 2 unilateral ruptures from the epicentre and one bilateral. We distinguish the "unfavourable" case, when at least one of the rupture scenario does not match the reference impact and the "favourable" case, when at least one matches the reference impact.

Four distinct cases are analysed in order to evaluate the performance depending on the options available:

- GHS classic: GHS database population with classic uncertainties (15km for the epicentre location and 0.2 for the magnitude).
- GHS reduced: GHS database population with reduced uncertainties (10km for the epicentre location and 0.1 for the magnitude).
- LandScan classic: LandScan database population with classic uncertainties.
- LandScan reduced: LandScan database population with reduced uncertainties.

The Tab. 4.1, 4.2 4.3, and 4.4 summarise the results of the performance analysis for these cases, while Tab. 4.5 presents the results before the upgrade (using the LandScan database and classic uncertainties).

Result	All		M<7	M $\geq$ 7	
	unfavourable	favourable		unfavourable	favourable
Correct	99.3%	99.5%	99.6%	76.3%	90.7%
Overestimation	0.2%	0.2%	0.1%	3.1%	3.1%
Underestimation	0.3%	0.3%	0.3%	6.2%	6.2%
Uncategorisable	0.2%	0.0%	-	14.4%	0.0%

Table 4.1: EQIA's performance (GHS classic) for 7291 earthquakes (7194  $M < 7$  and 97  $M \geq 7$ ) from January 2010 to May 2019.

As already noticed in the previous report, EQIA present very good performance. The different cases discussed here have similar to slightly better results than the previous version of EQIA, especially reducing the cases of overestimation for  $M > 7$  events.

As expected, when uncertainties are reduced, the forecasted impact presents an narrower range, resulting in lower performance while remaining excellent.

Concerning the use of different population database, while we do not know which one best represents the actual population density, the use of the GHS database lends slightly better results, especially when it comes

Result	All		M<7	M <sub>≥</sub> 7	
	unfavourable	favourable		unfavourable	favourable
Correct	98.7%	99.0%	99.2%	67.0%	86.6%
Overestimation	0.6%	0.6%	0.5%	5.2%	5.2%
Underestimation	0.4%	0.4%	0.3%	8.2%	8.2%
Uncategorisable	0.3%	0.0%	-	19.6%	0.0%

Table 4.2: EQIA's performance (GHS reduced) for 7291 earthquakes (7194 M<7 and 97 M<sub>≥</sub>7) from January 2010 to May 2019.

Result	All		M<7	M <sub>≥</sub> 7	
	unfavourable	favourable		unfavourable	favourable
Correct	98.9%	99.1%	99.3%	72.2%	84.5%
Overestimation	0.7%	0.7%	0.5%	10.3%	10.3%
Underestimation	0.2%	0.2%	0.2%	5.1%	5.1%
Uncategorisable	0.2%	0.0%	-	12.4%	0.0%

Table 4.3: EQIA's performance (LandScan classic) for 7291 earthquakes (7194 M<7 and 97 M<sub>≥</sub>7) from January 2010 to May 2019.

Result	All		M<7	M <sub>≥</sub> 7	
	unfavourable	favourable		unfavourable	favourable
Correct	98.0%	98.2%	98.4%	66.0%	79.4%
Overestimation	1.4%	1.4%	1.3%	14.4%	14.4%
Underestimation	0.4%	0.4%	0.3%	6.2%	6.2%
Uncategorisable	0.2%	0.0%	-	13.4%	0.0%

Table 4.4: EQIA's performance (LandScan reduced) for 7291 earthquakes (7194 M<7 and 97 M<sub>≥</sub>7) from January 2010 to May 2019.

Result	All		M<7	M <sub>≥</sub> 7	
	unfavourable	favourable		unfavourable	favourable
Correct	98.6%	98.7%	98.9%	74.5%	82.7%
Overestimation	1.0%	1.0%	0.8%	15.3%	15.3%
Underestimation	0.2%	0.2%	0.2%	2.0%	2.0%
Uncategorisable	0.1%	0.0%	-	8.2%	0.0%

Table 4.5: EQIA's performance before the upgrade (LandScan database, classic uncertainties) for 7268 earthquakes (7171 M<7 and 97 M<sub>≥</sub>7) from January 2010 to May 2019.

to  $M \geq 7$  earthquakes. As already mentioned, EQIA will produce visual outputs for both databases, in order to include this lack of knowledge in its impact assessment.

Due to the low statistics for  $M \geq 7$  earthquakes, it is hard to say whether the rupture length new evaluation is a compelling upgrade in terms of performance. However it seems a more suitable approach since it benefits from a more recent work, based on a bigger data-set.



## Conclusion

In addition to its transcription and update in Python, EQIA has been improved in various way to asses more realistic impact as well as account for new sources of uncertainties, in particular the one related to the population density around the epicentre.

This new version of EQIA present excellent performance, slightly better than the previous version with 99% of correct impact estimations (when uncertainties are of the same order), in particular when using the GHS database (99.5% of correct impact predictions with 76.3 to 90.7% for  $M \geq 7$  event depending on the rupture scenario).

As mentioned in this report, as part of the RISE project, some work will be conducted in the estimation of the fault rupture parameters from crowd-sourced data in collaboration with ETHzürich with the FinDer algorithm, that could be usefull as input for EQIA.





## A Execution time

On Fig. A.1 is displayed the execution time as a function of the magnitude for the same epicentre coordinates.

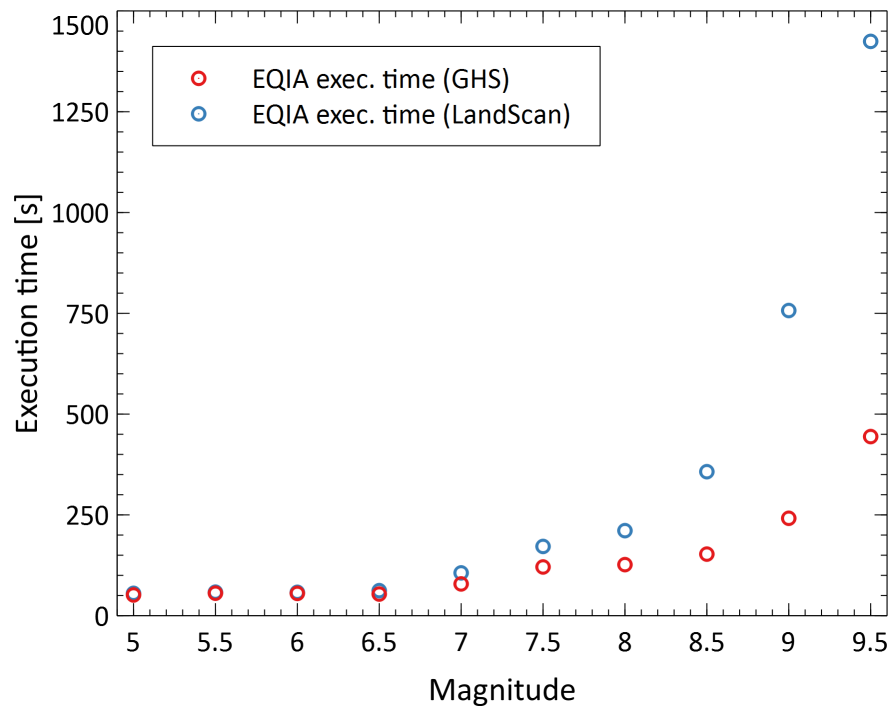


Figure A.1: Average EQIA execution times (over three executions) for the same epicentre coordinates (i.e. the same population distribution) with different magnitude and population databases. These numbers highly depend on the population distribution.

As the area impacted by the earthquake greatly increases with the magnitude, requests in the population databases are more and more costly. Since the GHS database suggests a denser population than the LandScan database, it has less entries. As a consequence, the database queries on GHS are much faster than on LandScan. For smaller magnitudes (roughly  $M < 7.0$ ), creating the visual outputs is the most time consuming part (thus we have a plateau at low amplitudes). The execution time depends mainly on the magnitude and on the region (populated or not).



## Bibliography

- [1] S. Julien-Laferrière et al., “Earthquake Qualitative Impact Assessment Performance Evaluation,” *SERA JRA6*, 2019.
- [2] M. Leonard, “Self-Consistent Earthquake Fault-Scaling Relations: Update and Extension to Stable Continental Strike-Slip Faults,” *B. Seismol. Soc. Am.*, vol. 104, no. 6, pp. 2953–2965, 2014.
- [3] J. Roger et al., “Applications and Utilization of ELER Software,” *NERIES JRA3-D5*, 2009.
- [4] S. Gilles et al., “Utilization of ELER V2 and Improvement of EMSC Earthquake Impact Estimation Method,” *NERIES JRA3-D5*, 2010.
- [5] Oak Ridge National Laboratory, “LandScan™ High Resolution global Population Data Set copyrighted by UT-Battelle, LLC, operator of Oak Ridge National Laboratory under Contract No. DE-AC05-00OR22725 with the United States Department of Energy,” accessed on May 2019. <https://landscan.ornl.gov>.
- [6] S. Freire et al., “Development of new open and free multi-temporal global population grids at 250 m resolution,” *AGILE*, 2016.
- [7] M. Schiavina, S. Freire and K. MacManus, “GHS population grid multitemporal (1975, 1990, 2000, 2015) R2019A,” 2019. <http://data.europa.eu/89h/0c6b9751-a71f-4062-830b-43c9f432370f>.
- [8] D. L. Wells and K. J. Coppersmith, “New Empirical Relationships among Magnitude, Rupture Length, Rupture Width, Rupture Area, and Surface Displacement,” *B. Seismol. Soc. Am.*, vol. 84, no. 4, pp. 974–1002, 1994.
- [9] P. Bird, “An updated digital model of plate boundaries,” *Electronic J. Earth Sci.*, vol. 4, no. 3, 2003.
- [10] National Centers for Environmental Information, accessed on May 2019. <https://www.ngdc.noaa.gov/hazard>.